ACS APPLIED MATERIALS & INTERFACES

Letter

www.acsami.org

Preparation of Dye-Adsorbing ZnO Thin Films by Electroless Deposition and Their Photoelectrochemical Properties

Satoshi Nagaya[†] and Hiromasa Nishikiori*[,‡]

[†]Nagano Prefecture General Industrial Technology Center, 1-3-1 Osachi-Katamacho, Okaya, Nagano 394-0084, Japan

[‡]Department of Environmental Science and Technology, Faculty of Engineering, Shinshu University, 4-17-1 Wakasato, Nagano 380-8553, Japan

ABSTRACT: Dye-adsorbing ZnO thin films were prepared on ITO films by electroless deposition. The films were formed in an aqueous solution containing zinc nitrate, dimethylamine–borane, and eosin Y at 328 K. The film thickness was 1.2–2.0 μm. Thinner and larger-plane hexagonal columns were produced from the solution containing a higher concentration of eosin Y. A photocurrent was observed in the electrodes containing such ZnO films during light irradiation. The photoelectrochemical performance of the film was improved by increasing the concentration of eosin Y because of increases in the amount of absorbed photons and the electronic conductivity of ZnO.

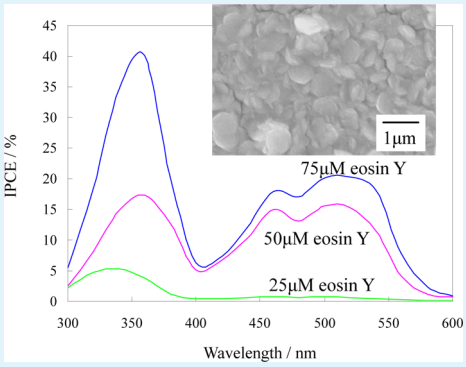

KEYWORDS: *ZnO, thin film, eosin Y, electroless deposition, photoelectric conversion, photoelectrochemistry*

1. INTRODUCTION

Zinc oxide (ZnO) is an interesting material because it can be conductive and semiconductive and its films can be prepared by electrodeposition[1,2] or electroless deposition[3,4] using a low-temperature process.

In the electrodeposition process using $Zn(NO_3)_2$, organic dye-adsorbing ZnO particles were spontaneously deposited from the solution containing the organic dye and $Zn(NO_3)_2$. Yoshida et al. prepared ZnO–dye (such as eosin Y and phthalocyanine) hybrid films from the aqueous solution by electrodeposition[5−7] and tested them for use as solar cells by investigating the photoelectrochemical properties of the films. This method can be developed by electronics industries for optical devices, etc., in the future because it can produce a device at low temperature and low cost and can be used to produce large-sized products.

On the other hand, the preparation of ZnO–dye hybrid films by electroless deposition has not been sufficiently studied. The rate of electroless deposition of ZnO is lower than that of electrodeposition because it progresses by only oxidation–reduction reactions using a reducing agent in the solution. Electroless deposition has hardly been used because it takes several hours to prepare a few-micrometer-thick ZnO film.[4] However, by electroless deposition, the films can also be prepared on nonconductive substrates, such as plastics, without any electric power source. Compared to electrodeposition, electroless deposition can easily prepare films consisting of nanosized particles that have a large specific surface area because of the slow deposition rate. Therefore, the films can be used for energy conversion devices highly sensitive to energy input, i.e., high-performance electroluminescence and photoelectric conversion devices, etc. Besides, it is important to study the influence of the dye–molecular species on the electroless deposition process of ZnO for the production of organic–inorganic hybrid films.

In this study, we prepared ZnO–eosin Y hybrid films by electroless deposition on conductive glasses and examined their optical and electrochemical properties.

2. EXPERIMENTAL SECTION

2.1. Linear Sweep Voltammetry (LSV). LSV of $Zn(NO_3)_2$ and dimethylamine–borane (DMAB) was conducted in aqueous solutions. An ITO glass plate (AGC Fabritech, 9 Ω $\square^{-1}$) adsorbing the palladium catalyst particles on the surface, a Ag/AgCl standard electrode, and a platinum plate were used for the working, reference, and counter electrodes, respectively. $Zn(NO_3)_2$ and DMAB were individually dissolved in distilled water at a concentration of 0.1 mol dm^{-3}, and $NaClO_4$ as the supporting electrolyte was added to them at a concentration of 0.1 mol dm^{-3}. All of the solutions were adjusted to pH 6 and underwent argon gas bubbling. The polarization curves of $Zn(NO_3)_2$ and DMAB were obtained using a potentiostat (HA-501G, Hokuto Denko).

2.2. Electroless Deposition. The ITO glass plates were coated with ca. 30-nm-thick ZnO thin films as a buffer layer[8] and used as the substrates. The buffer layer was prepared by dip-coating with 2-methoxyethanol containing 0.25 mol dm^{-3}

Received: July 3, 2013
Accepted: September 10, 2013
Published: September 10, 2013

   dx.doi.org/10.1021/am4026483 | *ACS Appl. Mater. Interfaces* 2013, 5, 8841–8844

zinc acetate and 0.0125 mol dm^{-3} 2-aminoethanol. After dip-coating, the substrates were heat-treated at 723 K for 30 min. The ITO surface resistance was 31 Ω $\square^{-1}$ after heating.

The substrates with the ZnO thin films were rinsed in a 20 g dm^{-3} Na_3PO_4 aqueous solution containing a surfactant along with ultrasonication for 5 min in order to defat on the surface. They were then immersed in an aqueous colloid solution prepared from tin chloride. $SnO_2 \cdot xH_2O$ was supported as an adsorbent on the substrate surface.[9] They were washed with distilled water and then successively immersed in a $AgNO_3$ solution and a $PdCl_2$ solution for 1 min each. Pd^{2+} was adsorbed on the surface. Finally, the Pd catalyst particles were produced by the DMAB reductant in the next process.

Electroless deposition of the dye-adsorbing ZnO films was conducted for 4 h using an aqueous solution containing 0.05 mol dm^{-3} $Zn(NO_3)_2$, 0.05 mol dm^{-3} DMAB, and 0−75 μmol dm^{-3} eosin Y. The solution was prepared under the condition of ca. pH 6 and kept at 333 K with stirring. After electroless deposition, the substrates were washed with distilled water and dried at 343 and 423 K each for 30 min. The film samples prepared from solutions containing 0, 25, 50, and 75 μmol dm^{-3} eosin Y were labeled E0, E25, E50, and E75, respectively.

The surface morphology, cross-sectional thickness, X-ray diffraction patterns, UV−vis absorption spectra, and photoelectrochemical properties of the samples were measured as described elsewhere.[10] The amount of eosin Y in the film was estimated as follows: The film was immersed in a 0.1 mol dm^{-3} KOH solution in order to dissolve eosin Y into the solution. The absorption spectrum of the solution was measured, from which the concentration of eosin Y in the film was estimated.

3. RESULTS AND DISCUSSION

3.1. Polarization Curves of $Zn(NO_3)_2$ and DMAB Solutions. Figure 1 shows the anodic and cathodic polarization curves of 0.1 mol dm^{-3} $Zn(NO_3)_2$ and DMAB solutions, respectively. The onsets of the anodic current of DMAB and the cathodic current of $Zn(NO_3)_2$ were observed to be ca. −0.45 and +0.30 V (vs Ag/AgCl), respectively. The potential at the intersection point was −0.35 V (vs Ag/AgCl). The formation process of ZnO is the same process as electrodeposition.[3]

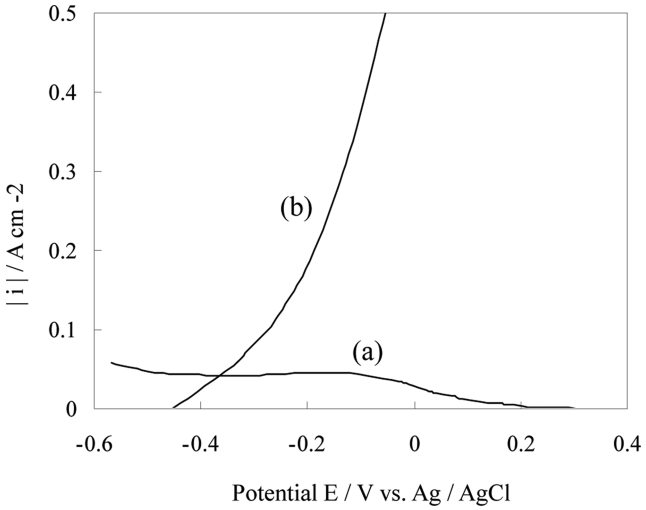

Figure 1. Electrochemical polarization curves of (a) $Zn(NO_3)_2$ and (b) DMAB solutions.

According to the mixed potential theory,[11] the intersection point of the partial cathodic and anodic polarization curves is the potential of this reaction. Therefore, it was suggested that the potential of the electroless reaction was −0.35 V (vs Ag/AgCl). The absolute potential value of electroless deposition was lower than that of electrodeposition because ZnO films are usually prepared by electrodeposition in a 0.1 mol dm^{-3} $Zn(NO_3)_2$ aqueous solution at −0.7 V (vs Ag/AgCl).[12] The slow rate of the electroless process is because the growth rate of the ZnO particles is slower at the lower absolute potential value.

3.2. Electroless Deposition of ZnO. E0 consisted of a white film, whereas E25, E50, and E75 were red because of the color of eosin Y in the solution. This is consistent with the hypothesis that ZnO and eosin Y were simultaneously deposited. Figure 2 shows SEM images of the surface and cross section of the samples. The surface morphology of the ZnO film depends on the concentration of eosin Y in the solution. The particle size was larger on the surface of the ZnO film prepared from the solution containing a higher concentration of eosin Y. In E0 and E25, there were large pores between the ZnO particles. The particles were more densely packed in the film containing a greater amount of eosin Y. The film thicknesses were evaluated from the cross-sectional images. As the concentration of eosin Y in the solution increased, the thickness of the film prepared from the solution decreased, opposite to the tendency of the particle size.

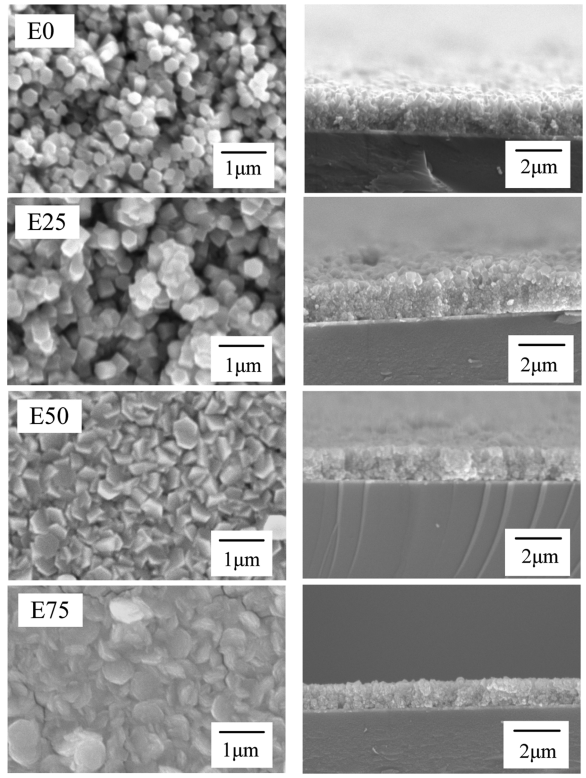

Figure 2. SEM images of the surface (left) and cross section (right) of E0, E25, E50, and E75.

Figure 3 shows X-ray diffraction patterns of the films. It was identified that the highly crystalline ZnO particles were deposited because all of the samples have sharp peaks. As the concentration of eosin Y decreased in the solution, the relative intensity of the (0002) peak was stronger in the films prepared

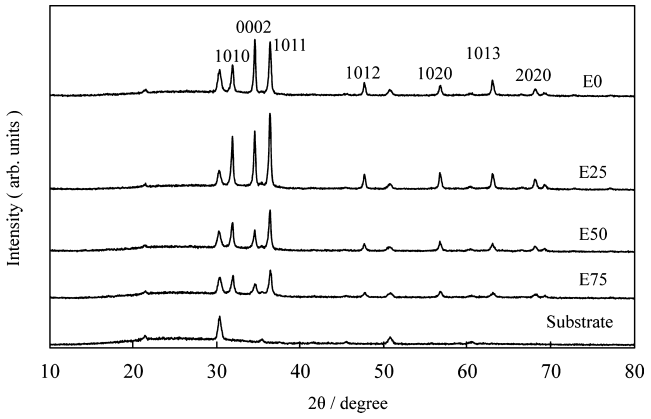

Figure 3. X-ray diffraction patterns of E0, E25, E50, and E75.

from the solution. This indicated that the particles with a hexagonal column structure of wurtzite-type ZnO grew along the *c* axis. The crystallite thickness was estimated from the full width at half-maximum of the (0002) peak using Scherrer's equation to be 42.3, 36.7, 33.9, and 22.9 nm for E0, E25, E50, and E75, respectively.

On the basis of the X-ray diffraction patterns, the crystals preferred to grow in the *c*-axis direction as the concentration of eosin Y in the solution decreased. The crystals spontaneously grow in the *c*-axis direction because the (0002) plane has the highest surface energy and polarity in wurtzite ZnO.[13] However, in the presence of eosin Y in the solution, the growth of ZnO in the *c*-axis direction was consequently prevented because the eosin Y molecules were preferentially adsorbed on the (0002) plane of ZnO.[14] Therefore, the ZnO particles were larger in the *a*- and *b*-axis directions and flake-shaped. Furthermore, the film thickness decreased because the particles were densely packed and oriented parallel to the substrate.

Figure 4 shows the absorption spectra of the samples. The absorbance at 450−550 nm increased with an increase in the

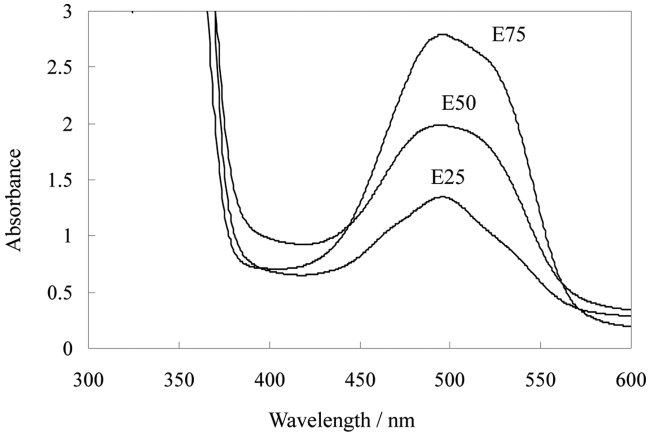

Figure 4. UV−vis absorption spectra of E25, E50, and E75.

concentration of eosin Y in the solution. The absorption peak at 500 nm and shoulder at around 530 nm were assigned to eosin Y. This result indicated that the amount of eosin Y in the films prepared from the solution increased with an increase in the concentration of eosin Y in the solution. The amount of eosin Y per unit thickness increased with an increase in the concentration of eosin Y because of the decrease in the film thickness.

The maximum absorbance per unit thickness (μm) was 0.66, 1.31, and 2.3 μm^{-1} for E25, E50, and E75, respectively. The amount of eosin Y in the film prepared from the solution drastically increased as the concentration of eosin Y in the solution increased. The amount of eosin Y in E75 was 2.3×10^{-8} mol cm^{-2}. The film thickness was 1.2 μm. Therefore, the concentration of eosin Y in the film was estimated to be 0.19 mol dm^{-3}. The absorption bands at 500 and 530 nm were assigned to the eosin Y dimer and monomer, respectively.[15] The amount of the dimer was estimated to be greater than that of the monomer in the films. These results indicated that the eosin Y molecules were competitively adsorbed on the ZnO surface when the ZnO crystals were deposited during electroless deposition. The dye molecules easily interacted with each other and were aggregated on the ZnO surface as the amount of dye in the solution increased.

Figure 5 shows the photocurrent action spectra and *I*−*V* curves of the electrodes. The incident photon-to-current efficiency (IPCE) value for E25 was quite low. The IPCE values increased depending on the amount of eosin Y in the film. The IPCE values at 500 nm were 0.7, 15, and 20 for E25, E50, and E75, respectively. A comparison of the IPCE and absorption spectra from 400 to 600 nm indicated that the current was generated by photoabsorption of eosin Y. The IPCE in the range from 300 to 400 nm increased with an increase in the concentration of eosin Y, and their maximum was 40% at 360 nm for E75.

The absorption edge of ZnO is ca. 375 nm because the optical band-gap energy of ZnO is 3.3 eV.[16] Therefore, the absorption from 300 to 400 nm depends on the ZnO band structure. However, the crystallinity of each film was not very different based on the X-ray diffraction patterns in Figure 3. The ZnO particles were larger and more densely packed in the film containing a higher concentration of eosin Y. The improvement of the IPCE in the range was due to an increase in the electronic conductivity of the ZnO film. The IPCE in the range from 400 to 600 nm increased with an increase in the dye amount. This is due to increases in the amount of the absorbed photons and the electronic conductivity of ZnO. Consequently, the photoelectric conversion efficiency also improved.

4. CONCLUSIONS

The eosin Y-adsorbing ZnO films were prepared on ITO substrates by electroless deposition from aqueous solutions containing $Zn(NO_3)_2$ and DMAB. The ZnO particle size in the film increased with an increase in the concentration of eosin Y in the solution. The amount of eosin Y in the film increased with an increase in the concentration of eosin Y in the solution. Thinner and larger-plane hexagonal columns were produced from the solution containing a higher concentration of eosin Y. It is suggested that the growth of ZnO in the *c*-axis direction was consequently prevented because the eosin Y molecules were preferentially absorbed on the (0002) plane of wurtzite ZnO. The film thickness decreased with an increase in the dye amount because the particles were densely packed and oriented parallel to the substrate. The photoelectrochemical performance of the film was improved by the increase in the concentration of eosin Y due to the increases in the amount of absorbed photons and the electronic conductivity of ZnO.

dx.doi.org/10.1021/am4026483 | ACS Appl. Mater. Interfaces 2013, 5, 8841−8844

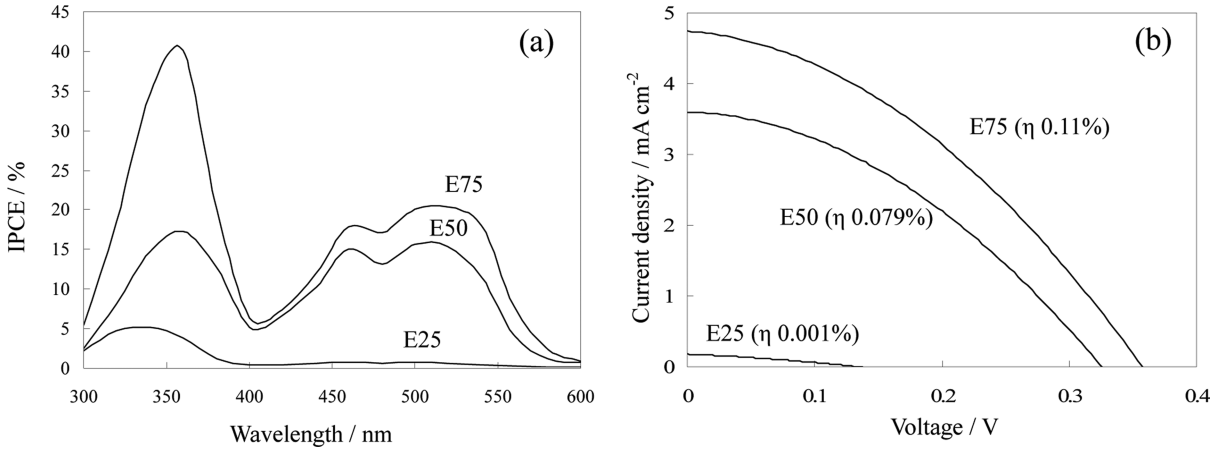

Figure 5. Photocurrent action spectra (a) and *I*–*V* curves (b) of E25, E50, and E75 (η = energy conversion efficiency).

AUTHOR INFORMATION

Corresponding Author

*E-mail: nishiki@shinshu-u.ac.jp.

Notes

The authors declare no competing financial interest.

REFERENCES

(1) Izaki, M.; Omi, T. *Appl. Phys. Lett.* **1996**, *68*, 2439−2440.
(2) Peulen, S.; Lincot, D. *J. Electrochem. Soc.* **1998**, *145*, 864−874.
(3) Izaki, M.; Omi, T. *J. Electrochem. Soc.* **1997**, *144*, L3−L5.
(4) Shinagawa, T.; Murase, K.; Otomo, S.; Katayama, J.; Izaki, M. *J. Electrochem. Soc.* **2009**, *156*, H320−H326.
(5) Yoshida, T.; Terada, K.; Schlettwein, D.; Oekermann, T.; Sugiura, T.; Minoura, H. *Adv. Mater.* **2000**, *16*, 1214−1217.
(6) Yoshida, T.; Minoura, H. *Adv. Mater.* **2000**, *16*, 1219−1222.
(7) Yoshida, T.; Tochimoto, M.; Schlettwein, D.; Wohrle, D.; Sugiura, T.; Minoura, H. *Chem. Mater.* **1999**, *11*, 2657−2667.
(8) Cameron, P. J.; Peter, L. M. *J. Phys. Chem. B* **2003**, *107*, 14394−14400.
(9) Lu, W.; Schmidt, H. *Adv. Powder Technol.* **2008**, *19*, 1−12.
(10) Nagaya, S.; Nishikiori, H. *Chem. Lett.* **2012**, *41*, 993−995.
(11) Power, G. P.; Ritchie, I. M. *J. Chem. Educ.* **1983**, *60*, 1022−1025.
(12) Izaki, M.; Omi, T. *J. Electrochem. Soc.* **1996**, *143*, L53−L55.
(13) Kong, X. Y.; Wang, Z. L. *Appl. Phys. Lett.* **2004**, *84*, 975−977.
(14) Wagata, H.; Ohashi, N.; Taniguchi, T.; Katsumata, K.; Okada, K.; Matsushita, N. *Cryst. Growth Des.* **2010**, *10*, 4968−4975.
(15) Rohatgi, K. K.; Mukhopadhyay, A. K. *Photochem. Photobiol.* **1971**, *14*, 551−559.
(16) Shinagawa, T.; Otomo, S.; Katayama, J.; Izaki, M. *Electrochim. Acta* **2007**, *53*, 1170−1174.